


ORIGINAL ARTICLE

Foxg1 Regulates the Postnatal Development of Cortical Interneurons

Wei Shen¹, Ru Ba ¹, Yan Su¹, Yang Ni¹, Dongsheng Chen¹, Wei Xie², Samuel J. Pleasure³ and Chunjie Zhao^{1,4}

¹Key Laboratory of Developmental Genes and Human Diseases, MOE, School of Medicine, Southeast University, Nanjing 210009, P. R. China, ²Key Laboratory of Developmental Genes and Human Diseases, MOE, Institute of Life Science, Southeast University, Nanjing 210009, P. R. China, ³Department of Neurology, Weill Institute for Neuroscience, Programs in Neuroscience and Developmental Stem Cell Biology, UCSF, San Francisco, CA 94158, USA and ⁴Center of Depression, Beijing Institute for Brain Disorders, Beijing 100069, People's Republic of China

Address correspondence to Chunjie Zhao, Key Laboratory of Developmental Genes and Human Diseases, School of Medicine, Southeast University, Nanjing 210009, China. Email: zhaocj@seu.edu.cn.  orcid.org/0000-0001-6601-2328,

Wei Shen and Ru Ba contributed to this work equally.

Abstract

Abnormalities in cortical interneurons are closely associated with neurological diseases. Most patients with Foxg1 syndrome experience seizures, suggesting a possible role of Foxg1 in the cortical interneuron development. Here, by conditional deletion of Foxg1, which was achieved by crossing Foxg1^{fl/fl} with the Gad2-Cre^{ER} line, we found the postnatal distributions of somatostatin-, calretinin-, and neuropeptide Y-positive interneurons in the cortex were impaired. Further investigations revealed an enhanced dendritic complexity and decreased migration capacity of Foxg1-deficient interneurons, accompanied by remarkable downregulation of Dlx1 and CXCR4. Overexpression of Dlx1 or knock down its downstream Pak3 rescued the differentiation defects, demonstrated that Foxg1 functioned upstream of Dlx1-Pak3 signal pathway to regulate the postnatal development of cortical interneurons. Due to the imbalanced neural circuit, Foxg1 mutants showed increased seizure susceptibility. These findings will improve our understanding of the postnatal development of interneurons and help to elucidate the mechanisms underlying seizure in patients carrying Foxg1 mutations.

Key words: CXCR4, Dlx1, Foxg1, interneuron, migration

Introduction

The malformation of neural circuits is usually associated with mental illnesses, such as schizophrenia, autism, and epilepsy (Kann 2016). Although inhibitory interneurons only account for 15–20% of the cortical neurons (Meyer et al. 2011), the abnormal lamination of interneurons impairs the balance of the neural circuit. During the development, cortical interneurons are generated in the medial ganglionic eminence (MGE) and caudal ganglionic eminence (CGE) of the subpallium and migrate tangentially to the cortex at perinatal stages (Anderson et al. 2001;

Jimenez et al. 2002). After birth, cortical interneurons switch their tangential migration to radial and eventually arrive at their final destinations, where they establish connections with local target neurons (Ang et al. 2003; Tanaka et al. 2003, 2006, 2009; Martini et al. 2009). Among MGE-derived interneurons, somatostatin (SST)-positive interneurons prefer to be located in the deeper layers and in close proximity to excitatory neurons born during the same developmental window, while PV-positive interneurons distribute to the whole cortex except layer I (Valcanis and Tan 2003; Butt et al. 2005; Miyoshi et al.

2007); CGE-derived interneurons are located in the upper layers despite their birth date, thus forming the distinct lamination patterns of specific cortical interneuron subtypes (Pla et al. 2006; Miyoshi et al. 2010; Vucurovic et al. 2010; Miyoshi and Fishell 2011).

Although the embryonic development of cortical interneurons has been well explored over the last decade, the mechanisms underlying postnatal development of cortical interneurons are poorly understood. The C-X-C chemokine receptor 4 (CXCR4) has recently been shown to be required for the migration of cortical interneurons. Deficiency of CXCR4 results in an abnormal cortical distributions of SST, calretinin (CR)-, and neuropeptide Y (NPY)-positive interneurons, suggesting CXCR4 not only plays an important role in early embryonic but also may essentially function on postnatal developing cortical interneurons (Tiveron et al. 2006; Li et al. 2008; Tanaka et al. 2010; Meechan et al. 2012). Distal-less homeobox 1 (Dlx1) has been reported to regulate the differentiation by affecting interneuron neurite growth. Dlx1 knock down results in an advanced dendritic growth in vitro in response to upregulated Pak3 expression (Dai et al. 2014). Although much effort has been made, the molecular mechanism upstream of CXCR4 and Dlx1 to control the development of cortical interneurons needs to be further elucidated.

Previously, we have shown the Forkhead transcription factor Foxg1 has an essential function during the tangential migration of cortical interneurons (Yang et al. 2017). However, due to the embryonic lethality of *Dlx5/6-cre; Foxg1^{fl/fl}* mice, the postnatal role of Foxg1 was unable to be determined. In the present study, *Gad2-Cre^{ER}* mice were employed to specifically disrupt Foxg1 postnatally. After Foxg1 deletion, we found the laminar distributions of interneuron subtypes, including SST-, NPY-, and CR-positive interneurons in the cortex were impaired; furthermore, their migration capacity was significantly reduced, combined with a substantially decreased CXCR4 level. In Foxg1-deficient cortical neurons, Dlx1 expression was detected to be downregulated, resulting in remarkably enhanced dendrite overgrowth and increased complexity of neural processes. Interestingly, Foxg1-deficient mice exhibited an increased susceptibility to epilepsy. Our study explained, to a certain extent, why patients with Foxg1 syndrome have a high incidence of seizures. Taken together, these findings will help to further understand the molecular control of the development of cortical interneurons and the mechanisms of Foxg1 Syndrome.

Materials and Methods

Animals

The *Gad2-Cre^{ER}* line was purchased from the Jackson Laboratory, and the *Foxg1^{fl/fl}* line was generated as previously described (Tian et al. 2012). The conditional deletion of Foxg1 in postnatal developing interneurons was achieved by crossing the *Gad2-Cre^{ER}* with the *Foxg1^{fl/fl}* mice and combined with tamoxifen induction. 2% Tamoxifen was administered at postnatal day 1 (P1) afternoon at a dose of 5 μ L/g body weight. The Ai9 line was a

gift from Professor Xiaoming Li at Zhejiang University, the Gad67-GFP line was from Professor Yuchio Yanagawa at Gunma University, and the *Dlx5/6-cre-EGFP* line from Professor Zhengang Yang at Fudan University. The day of birth was designated as postnatal day P0. All animals were bred in the animal facility at Southeast University. No obvious differences were detected in either sex. All experiments were performed according to the approved guidelines of Southeast University.

Immunostaining

Brains were fixed by transcardial perfusion with cold 4% paraformaldehyde (PFA) after the animals were deeply anesthetized with pentobarbital sodium (50 mg/kg). The brains were then post fixed overnight, cryoprotected in 30% sucrose, embedded in optimum cutting temperature (OCT) compound and stored at -70°C until further use. The brains were cryosectioned into 16- μ m thick sections using a Leica CM 3050S cryostat. Immunostaining was then performed as previously reported (Tian et al. 2012). The following antibodies were used: rabbit anti-Foxg1 (Abcam, 1:1000); rat anti-bromodeoxyuridine (BrdU) (Abcam, 1:1000); rabbit anti-Calretinin (Abcam, 1:1000); chicken anti-GFP (Abcam, 1:1000); mouse anti-Reelin (Millipore 1:500); mouse anti-parvalbumin (Millipore, 1:1000); rabbit anti-CXCR4 (Abcam 1:500); rat anti-COUP-TF interacting protein 2 (CTIP2) (Abcam, 1:1500); rat anti-SST (Millipore 1:500); and mouse anti-neuronal nuclei (NeuN) (Millipore 1:500); Rabbit anti- Neuropeptide Y (NPY) (Sigma 1:500); goat anti-VIP (Santa cruz 1:500).

In Situ Hybridization

Brains were harvested as described above, with that phosphate buffered saline and 30% sucrose were prepared using diethylpyrocarbonate (DEPC)-treated water. In situ hybridization was performed as previously described (Zhao et al. 2006; Hu et al. 2014). The information of SST, NPY, and VIP probes is listed in Table 1.

Real-time PCR

The total RNA was isolated from the P2 cortex using the RNeasyPlus Mini Kit (Qiagen, 74104), according to the manufacturer's instructions. Each sample was reversely transcribed using MultiScribe reverse transcriptase (Fermentas, EP0441). Quantitative real-time PCR was performed using the SYBR Green fluorescent master mix (Roche, 4913914001) on a StepOne Plus Real-Time PCR System (Applied Biosystems). Primer information is listed in Table 2. Relative gene expression levels were normalized to the expression of the most reliable endogenous gene (glyceraldehyde 3-phosphate dehydrogenase, GAPDH). Three paired littermate brains were obtained from 3 different litters for the quantitative real-time PCR analysis. The data from mutant and control cultures were statistically analyzed using Student's t-test.

Table 1 Primers used to synthesize the probes used for in situ hybridization

Name	Forward	Reverse
SST	CCGGAATTCACGCTACCGAAGCCGTC	ACGCGTCGACGGGGCCAGGAGTTAAGGA
NPY	TCTCACAGAGGCCACCC	TTTTGAATGCATGGTACTTT
VIP	CGGAATTC	GCGTCGAC
	CCTGGCATTCTGATACTCTTC	ATTCTCTGATTCAGTCTGCCC

Table 2 Primers used for real-time PCR

Name	Forward	Reverse	Tm (°C)
CXCR4	GTGGATGGTGGTGTTC AATTC	CTTGGAGTGTGACAGCTTAGAG	60
Dlx1	ACGGGCTCTGGTGCAAGATCTAAT	AAAGCATCGGGTTACAGCCACAC	60
Pak3	CACCAAGACCAGAGCATACAA	CAGCAGAAGGTGGGATATCTTC	60

Western Blot

Dorsal cortices were collected at P2, and prepared as described previously (Guo et al. 2017). The primary antibodies used in this study were: goat-anti Pak3 (Santa Cruz Biotechnology, 1:500), rabbit anti-CXCR4 (Abcam, 1:100), rabbit anti-Foxg1 (Abcam, 1:1000), rabbit anti-Dlx1 (Sigma, 1:250) and rabbit anti-GAPDH (Cell Signaling Technology, 1:1500).

Cell Culture and Quantification of Dendrite Growth

Mouse primary cortical neurons were prepared from the *Gad2-Cre^{ER}*; *Foxg1^{fl/fl}*; Ai9 (mutants) and the *Gad2-Cre^{ER}*; *Foxg1^{fl/+}*; Ai9 (heterozygous) mice. P2 mice were anesthetized and decapitated 24 h after tamoxifen administration. Brains were dissected in ice-cold HBSS (Invitrogen), and dorsal cortices were isolated and digested with 0.125% trypsin (Invitrogen) for 8 min at 37 °C, followed by neutralization with 2 ml of DMEM supplemented with 10% FBS, 1% GlutaMAXTM-1 and 0.2% penicillin/streptomycin (all obtained from Invitrogen). Cortices were then dissociated by pipetting and the suspensions were centrifuged at 1000 rpm for 5 min. The cells were resuspended, plated at a density of 4×10^4 cells/cm² and cultured in Neurobasal medium supplemented with 2% B27, 1% GlutaMAXTM-1 and 0.2% penicillin/streptomycin (all obtained from Invitrogen).

Interneurons were cultured for 3 and 7 days in vitro (DIV) to quantify dendrite growth. At 3 DIV and 7 DIV, the total dendrite length and the number of dendritic branches were measured using the Sholl analysis method with ImageJ. The number of dendritic intersections in concentric circles with various radii from the centroid of the soma was counted and plotted against the distance from the soma of the tdTomato⁺ interneurons. The significance of the differences in total dendrite length and the longest dendrite was compared using Student's *t*-test. The significance of the differences in complexity was determined using GraphPad Prism software with a two-way repeated-measures analysis of variance (ANOVA; genotype and circle radius as factors) followed by the Bonferroni post hoc test. We sampled 10 tdTomato⁺ interneurons from each genotype. This procedure was repeated in 3 separate experiments for a total of 30 mutant or control neurons analyzed.

Viral Transfection In Vitro

The cultured dorsal cortex neurons were transfected by using the lentiviral vectors containing the Dlx1 overexpressing vector or the Pak3 shRNA vector. Full-length Dlx1 sequence was cloned to produce the LV-Dlx1. The LV-Dlx1-EGFP and the control (Ubi-MCS-EGFP) were constructed and synthesized by Shanghai GeneChem Co., Ltd. (Shanghai, China). A shRNA plasmid was constructed to knock down Pak3. The targeting sequence of Pak3 was 5'-TAGCAGCACATCAGTCAATA-3' by using (sense strand 5'-GATCCGTAGCAGCACATCAGTCAATATTCAAGAGATATTAGACTGATGTGATGCTATTTTTGGAAA-3'; antisense strand:5'-AGCTTTTCCAAAAAATAGCAGCACATCAGTCAATATCTCTTGAATATTCGACTGATGTGCTGCTACG-3'). The

LV-Pak3-shRNA-gcGFP and the control (hU6-MCS-gcGFP) were constructed and synthesized by Shanghai GeneChem Co., Ltd. (Shanghai, China). The cultured dorsal cortex neurons were transfected at DIV1 by adding to the culture media directly which the titer MOI was 1 and the transfection media were changed after 24 h. Then cells were cultured in neural basal media for sholl analyze at DIV 7.

Time-Lapse Imaging and Analysis

Cortical slices were cultured as previously reported (Tanaka et al. 2003). Briefly, brains were removed from the P2 *Gad2-Cre^{ER}*; *Foxg1^{fl/fl}*; Ai9 (mutants) and the *Gad2-Cre^{ER}*; *Foxg1^{fl/+}*; Ai9 (heterozygous), dissected and embedded in 4% low-melting-point agarose. Coronal sections of 150 μm were obtained using a vibrating microtome (VT1000; Leica Microsystems) and deposited onto a poly-L-lysine-coated Millicell CM membrane (Millipore). Slices at the level containing the striatum, but not the hippocampus and the corpus callosum, were selected. Cortical slices were immersed in Neurobasal culture media and incubated in a 37 °C chamber with 5% CO₂. The time-lapse analysis (15-min intervals for 480 min) was performed on an EVOS FL auto with a live cell imaging system (Life Technologies), and approximately 9 sections (60 μm) were obtained, with an optional Z-stack. The images were taken in the field of somatosensory cortex. For the quantitative analysis of the migration distance, total 1087 or 1282 neurons from 8 or 9 brain slices obtained from 3 paired littermates were analyzed for mutants or controls, respectively, and the cumulative distance was defined as the sum of the distance of each step, whereas the overall distance was defined as the distance from the beginning position to the final position. Migration efficiency = overall distance/cumulative distance (Inamura et al. 2012). The data from the mutant and control slices were statistically analyzed using Student's *t*-test.

PTZ Administration and Seizure Score

Mice were subcutaneously injected with 50 mg/kg pentylenetetrazole (PTZ; Sigma, dissolved in 0.9% NaCl 50 mg/mL), immediately placed in a cage and monitored for 30 min by observers who were blind to genotypes. Thirteen control and 11 mutant mice were employed in this experiment. Seizures were scored according to a modified Racine scale designed specifically for PTZ-induced seizures in mice (Naydenov et al. 2014).

Microscopy and Image Analysis

Sections were viewed under a confocal microscope (Olympus FV1000), and the images were collected and analyzed using FV10-ASW image analysis software. The images were optimized for size, color, and contrast using Adobe Illustrator.

Statistical Analysis

Student's *t*-tests were performed to compare the lamination of cortical interneurons. The cortex, spanning from the pial

surface to white matter was divided into 10 equal bins (layer I spanned bin 1; layer II/III spanned bins 2–3; layer IV spanned bins 4–5; layer V spanned bins 6–7, and layer VI spanned bins 8–10), and the number of interneurons was calculated by an investigator who was blinded to the genotypes. Three paired littermate brains were obtained from 3 different litters. Mouse genders were not determined. Statistical tests were performed with GraphPad Prism 5.0. Differences were considered significant at $P < 0.05$.

Results

Decreased Number and Abnormal Distribution of Cortical Interneurons after Postnatal Deletion of *Foxg1*

As shown in our previous study, *Foxg1* regulates the tangential migration of cortical interneurons during embryonic development. Due to embryonic death of *Dlx5/6-cre;Foxg1^{fl/fl}* mice, the role of *Foxg1* in postnatal development of cortical interneurons was unable to be determined. Here, *Gad2-Cre^{ER}* line was employed to conditionally delete *Foxg1* during postnatal development to elucidate its potential function. We first examined the recombination efficiency of Cre in *Gad2-Cre^{ER};Ai9* cortex by immunostaining for anti-parvalbumin (PV), anti-somatostatin (SST), anti-calretinin (CR), anti-Reelin, anti-neuropeptide Y (NPY), and anti-vasoactive intestinal protein (VIP), the specific markers for distinct cortical interneuron subtypes (Gelman and Marin 2010). As shown in Figure 1A–F, after tamoxifen administration at P1, recombination occurred in almost all subtypes of cortical interneurons upon examination at P14. Next we detected the efficiency of *Foxg1* deletion. As shown in Figure 1G–H', at P2, 1 day after TM administration, the protein level of *Foxg1* was already either obviously decreased or undetectable in tdTomato⁺ cells. At P7, *Foxg1* was thoroughly deleted compared with the controls (Fig. 1I–J'). We then observed the number and lamination of interneurons at P2 and found that there were less tdTomato⁺ cells located at upper layers and more in the deeper region in mutants (Fig. 1K–M), while the number of tdTomato⁺ cells was comparable to that of *Gad2-Cre^{ER};Foxg1^{fl/+};Ai9* controls (Fig. 1N). In adult, the similar distribution defect was detected, but the number of cortical interneurons was obviously decreased in mutants (Fig. 1O–R). Immunostaining of anti-Caspase 3 was then performed to detect cell apoptosis. No significant statistic changes was observed (data not shown), possibly due to a gradual, slow loss.

Previous studies have shown that cortical interneurons are heterogeneous and are derived from the ventral ganglionic eminence (GE) and can be classified by their morphologies and specific markers (Gelman and Marin 2010; Bartolini et al. 2013). Dorsal MGE-derived interneurons mainly express SST, and most ventral MGE-derived interneurons express PV (Wonders et al. 2008). SST-positive interneurons are preferentially located in the deeper cortical layers, while the PV-positive interneurons distributed in the whole cortex except layer I and both of the subtypes are in close proximity to the excitatory neurons generated during the same developmental period (Valcanis and Tan 2003; Pla et al. 2006; Rymar and Sadikot 2007). The CGE-derived interneurons are usually concentrated within the upper layers, regardless of their birth date (Rymar and Sadikot 2007; Miyoshi et al. 2010). We examined the lamination of MGE- and CGE-derived interneurons by *in situ* hybridization for SST, VIP, and NPY, as well as immunostaining for PV, CR, and Reelin. As shown in Figure 2A–C, the majority of SST-positive interneurons is tend to be located in the deeper layers in the controls

(Fig. 2A,A'); however, an increased percentage of SST-positive interneurons was observed in upper layer II/III, accompanied by a decrease in deeper layer V in the mutants (Fig. 2B,B',C). The lamination of PV-positive interneurons in mutants seemed to be comparable to that in the controls, and no obvious changes were detected (Fig. 2D–F). Since, CR and NPY are also expressed in subtypes of MGE-derived SST-positive interneurons, we further investigated the distributions of these subtypes. The CR-positive cells were mainly located in the upper layers in the controls, but more CR-positive cells were detected in the deeper layers in the mutants (Fig. 2G–H'). Surprisingly, many ectopic CR-positive cells were observed in the layers VI (Fig. 2H, H', I). A slight increase in the number of NPY-positive interneurons was detected in layer V of the mutants compared with that of the controls, in which NPY-positive interneurons were mainly located in layers II–IV, VI, with only a few in layer V (Fig. 2J–L). We next examined the CGE-derived VIP- and Reelin-positive interneurons. No obvious distribution abnormalities were observed for these 2 subtypes (Fig. 2M–R). Thus, postnatal ablation of *Foxg1* led to a decreased number of cortical interneurons and abnormal distributions of SST-, CR-, and NPY-positive but not PV-, VIP-, and Reelin-positive interneurons, indicating that *Foxg1* plays an important role in the postnatal development of cortical interneurons.

The Ectopic CR-Positive Interneurons Were Generated Postnatally

Since CR is expressed in several types of neurons, including cortical interneuron subtypes and pyramidal excitatory neurons in layer Vb (Liu et al. 2014), we examined the ectopic CR-positive cells by double immunostaining for anti-CR and CTIP2, a specific marker for deeper layer excitatory neurons (Chen et al. 2008). As shown in Figure 3A,B, none of the CR-positive cells co-expressed CTIP2, suggesting that the ectopic CR-positive cells were not excitatory neurons. To further identify the CR-positive cells, a *Gad67-GFP* line in which most cortical interneurons labeled by GFP was employed (Tamamaki et al. 2003). As shown in Figure 3C,D, all of the CR-positive neurons were GFP-positive, indicating that the ectopic CR-positive cells were interneurons. It has been reported that although the majority of cortical interneurons are generated at embryonic stages, a small proportion has been reported to be generated postnatally (Riccio et al. 2012). To determine when the ectopically distributed CR-positive interneurons were generated, a birth-dating experiment was performed. Because some CR-positive interneurons shared the same identity as SST-positive interneurons (Xu and Callaway 2009), we first administered BrdU at E12.5, the time point at which the SST-positive interneurons are primarily generated. When examine at P14, none of the ectopic CR-positive interneurons were found to be BrdU-positive (Fig. 3E,E'). The same results were obtained when BrdU was given at E13.4 and E14.5 (Fig. 3F,F'). When BrdU was injected at E15.5, the time at which the CGE-derived CR-positive interneurons are mainly generated, no co-localization of CR with BrdU was detected either (Fig. 3G,G'). Taking together, the CR-positive interneurons were not produced embryonically and their accumulation in the deeper layers was not due to a cell fate switch of MGE- or CGE-derived interneurons. Since an interneuron progenitor pool has been identified in the white matter and shown to continuously generate cortical CR-positive interneurons during the first 2 postnatal weeks (Riccio et al. 2012), BrdU was then administered 3 times at P1, P5, and P10 to explore the properties of the ectopic CR-positive interneurons.

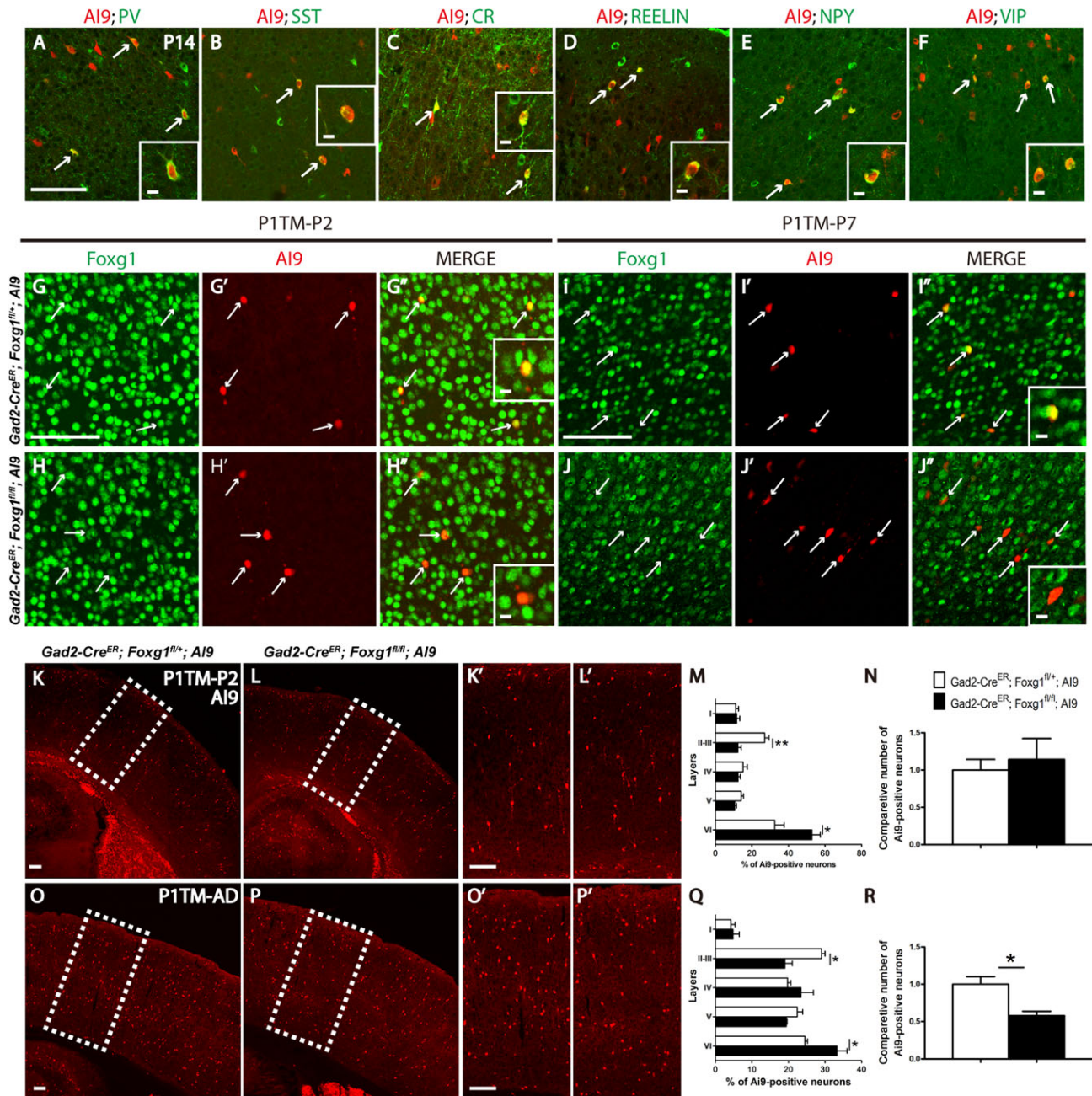


Figure 1. Postnatal disruption of *Foxg1* decreased the total number of cortical interneurons. (A–F) Cre-mediated recombination occurred in most of the cortical interneuron subtypes in *Gad2-Cre^{ER};Ai9* mice. tdTomato was detected in PV-, SST-, CR-, Reelin-, NPY-, VIP-positive interneurons (arrows) when tamoxifen was administered at P1 and the mice were examined at P14. (G–H^{''}) At P2, compared with the controls (G–G^{''}), the protein level of *Foxg1* was either decreased or undetectable after TM was given at P1 (H–H^{''}). (I–J^{''}) At P7, *Foxg1* expression was efficiently deleted in the tdTomato-positive interneurons in the mutants. Inserts in G^{''}, H^{''}, I^{''}, J^{''} indicate the high magnification views of double-labeled interneurons. (K–R) The distribution of tdTomato⁺ interneurons was disrupted in mutant while no obvious alterations in the total number of interneurons were detected at P2 (Control, n = 4; Mu, n = 3; P = 0.0643; layer II–III, P = 0.0059; layer VI, P = 0.0361 when tamoxifen was administered at P1; however, the ablation of *Foxg1* caused a decrease in the interneuron number in the adult and a similar abnormal distribution of tdTomato⁺ interneurons (M–P; Control, n = 3; Mu, n = 3; P = 0.0237; layer II–III, P = 0.0108; layer VI, P = 0.0366). Scale bar: 100 μm. Scale bar in inserts: 10 μm. Student's t-test, *P < 0.05.

As shown in Figure 3H–H', many ectopic CR-positive interneurons were BrdU-positive, indicating that these cells were born postnatally and mislocalized in the deeper layers. The percentage of CR⁺ BrdU⁺ interneurons among total BrdU⁺ in the deeper layer was about 11% in mutants; in contrast, few co-localization was observed in the controls (Fig. 3I). Since olfactory bulb interneurons are produced continuously after birth and migrate to their destinations through RMS in the cortex (Lledo et al. 2008).

These postnatally born CR⁺ interneurons with migration defects might also be olfactory bulb interneurons.

The Migration Ability of Cortical Neurons Was Impaired After *Foxg1* Ablation

The correct lamination of cortical interneurons requires multiple precisely controlled events, which include the switch from

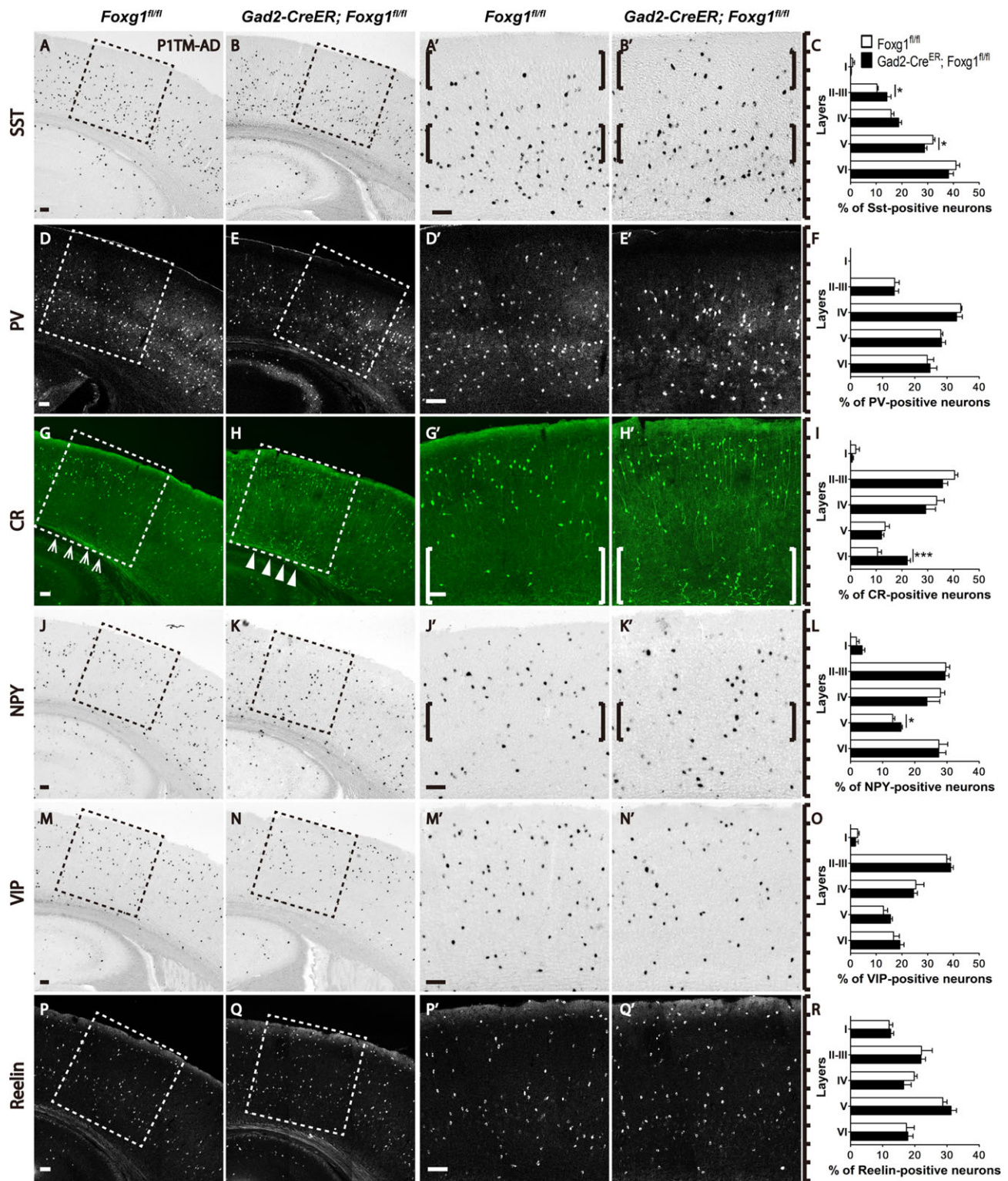


Figure 2. The SST-, CR-, NPY-positive subtype interneurons exhibited abnormal distributions in the adult cortex after *Foxg1* ablation. (A–C) SST-positive interneurons were preferentially located in the deeper layers in the controls (A, A', C), but more SST-positive interneurons were located in upper layer II–III, with a decreased number in layer V (B, B' C; Control, $n = 5$; MU, $n = 4$; layer II–III, $P = 0.0341$; layer V, $P = 0.0316$). (D–F) The distribution of PV-positive interneurons in the mutants (E, E', F) was not altered compared with the controls (D, D', F; Control, $n = 5$; MU, $n = 4$). (G–I) More CR-positive interneurons accumulated in the deeper layers in the mutants (H, H', I) than in the controls (G, G', I; Control, $n = 5$; MU, $n = 4$; layer VI, $P = 0.0006$). (J–L) More NPY-positive interneurons were distributed in layer V in the mutants (K, K', L; Control, $n = 3$; MU, $n = 3$; layer V, $P = 0.0265$). (M–R) No alterations were detected in the distributions of VIP-positive interneurons (M–O; Control, $n = 4$; MU, $n = 4$) and Reelin-positive interneurons (P–R; Control, $n = 4$; MU, $n = 4$). A', B', D', E', G', H', J', K', M', N', P' and Q' show higher magnification images of the boxed areas in A, B, D, E, G, H, J, K, M, N, P and Q, respectively. Scale bar: 100 μm . Student's *t*-test, * $P < 0.05$, ** $P < 0.01$.

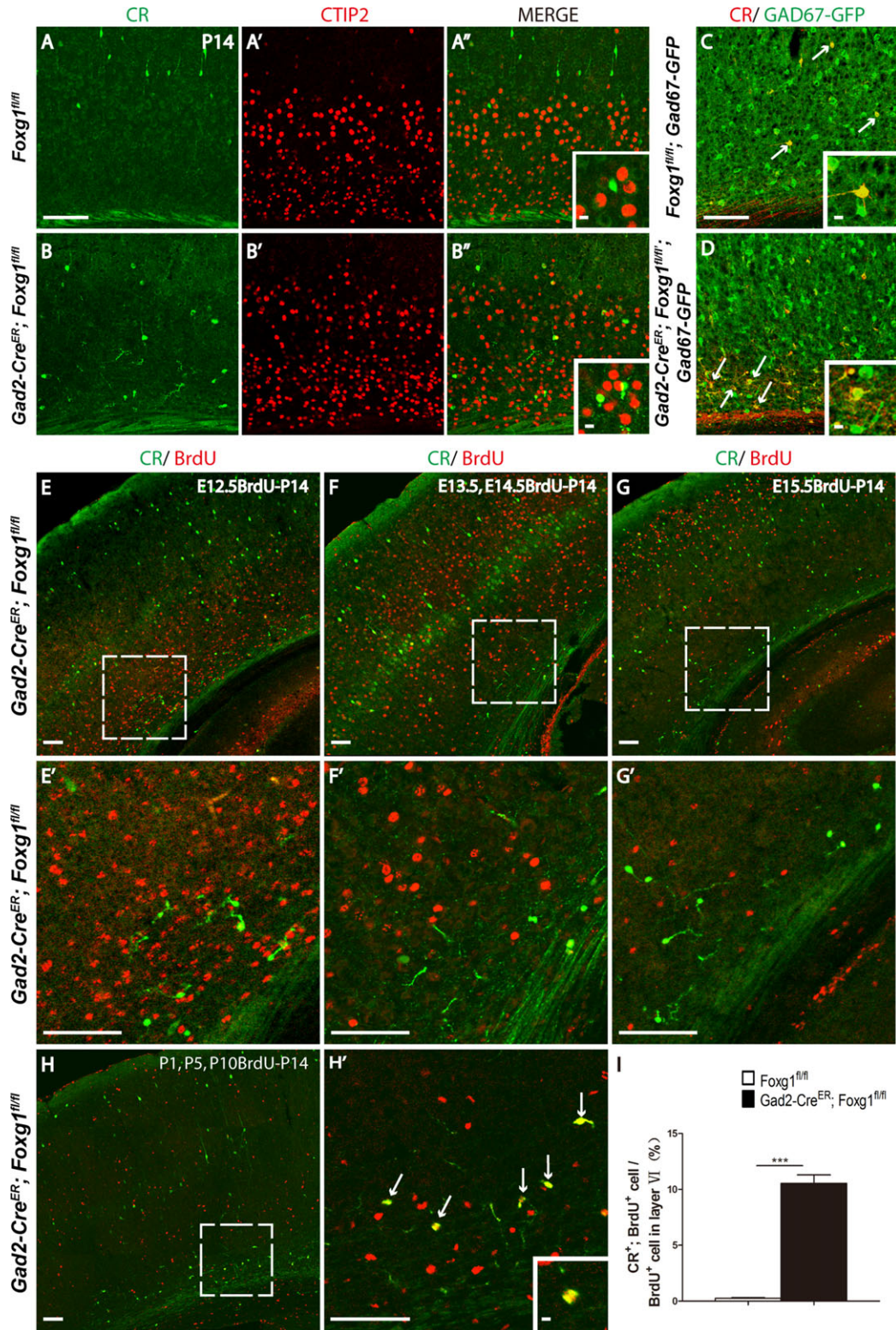


Figure 3. The ectopic CR-positive cells located in deeper layers are postnatally born interneurons. (A–B') The ectopic CR-positive cells located in the deeper layers of the mutants did not express the excitatory neuron marker CTIP2. Insert in A' and B' indicates the high magnification views. (C–D) These cells express GFP (arrows) in the *Gad2-Cre^{ER}; Foxg1^{fl/fl}; Gad67-GFP* mice, which labels interneurons. Insert in C and D indicate the high magnification views. (E–G) The deeper layer ectopic CR-positive interneurons were not generated at E12.5 (E), E13.5–E14.5 (G), or E15.5 (F). (H–H') Three BrdU injections at P1, P5 and P10 labeled most of the ectopic CR-positive deeper layer interneurons (arrows in H'), indicating that these interneurons were born postnatally. E', F', G', H' show higher magnification images of the boxed area in E, F, G, H. (I) The ratio of CR, BrdU double-positive cells among BrdU cells in Layer VI (I) was increased in mutant mice. (Control, n = 2; MU, n = 3, P < 0.0001). Scale bar: 100 μ m. Insert in H' indicate the high magnification views of double-labeled cells. Scale bar in inserts: 10 μ m. Student's t-test, ***P < 0.001.

tangential to radial migration, the radial migration, and accurate termination at their destinations (Faux et al. 2012). Since the deletion of *Foxg1* occurred after P1, when the switch from tangential to radial migration was almost completed, the abnormal distribution of cortical interneurons was more likely to be caused by an impaired migration capacity. A time-lapse analysis of interneurons labeled by tdTomato in cultured slices was then performed. Brain slices were dissected at P2 and observed for 480 min. As shown in Figure 4A,B, tdTomato⁺ interneurons that migrated shorter distances were marked by yellow arrowheads and interneurons that migrated longer distances by blue arrows. In mutants there are much more tdTomato⁺ interneurons migrated a shorter distance. We further statistically analyzed the migration capacity as previously described (Inamura et al. 2012) and found that the average cumulative migration distance of mutant interneurons was significantly decreased to $36.83 \pm 1.648 \mu\text{m}$ compared with $49.28 \pm 4.72 \mu\text{m}$ in the controls (Fig. 4C). Moreover, the overall migration distance was decreased from $27.06 \pm 4.09 \mu\text{m}$ to $15.89 \pm 1.39 \mu\text{m}$ (Fig. 4D). We then calculated the migration efficiency and observed a decrease from $52.76 \pm 3\%$ to $42.92 \pm 2.8\%$ (Fig. 4E), suggesting that mutant interneurons exhibited a more random migration pattern than that of the controls. The proportion of tdTomato⁺ interneurons that migrated short distances was significantly increased, meanwhile the proportion of interneurons migrated a long-distance was reduced in mutants (Fig. 4F,G). Based on our results, the *Foxg1* deletion impaired the migration capacity of interneurons.

As a classic receptor for Cxcl12, CXCR4 is well known to keep embryonic interneurons migrating along the tangential route and prevent from pre-invasion into the cortical plate (Stumm et al. 2003; Li et al. 2008; Wang et al. 2011). However, CXCR4 is also found to be expressed in interneurons in postnatal cortex when tangential migration is finished and Cxcl12 is thought no longer functions as a chemoattractant (Stumm et al. 2003, 2007; Li et al. 2008). Conditional disruption of CXCR4 at E16.5, the time point that radial migration is initiated results in severe lamination defects of SST, CR, and NPY-positive interneurons, suggesting the possible role of CXCR4 in radial migration which might be independent of Cxcl12 (Tanaka et al. 2010). Particularly, the ectopically located CR-positive interneurons show an analogous phenotype to our mutants (Li et al. 2008). We performed immunostaining of CXCR4 at P2 in the *Dlx5/6-Cre-EGFP* mice in which most of the cortical interneurons are labeled by EGFP and found out that CXCR4 is not only strongly expressed in interneurons on the tangential migration stream (Fig. 4H,1), but also in interneurons that the radial migration is already initiated (Fig. 4H2-5). Furthermore, in our mutants, the mRNA level of CXCR4 examined by Q-PCR and protein level detected by western blot and immunostaining were remarkably decreased (Fig. 4I-M). Thus, *Foxg1* may function upstream of the CXCR4 signaling pathway to control postnatal development of cortical interneurons.

***Foxg1* Is Involved in the *Dlx1*-*Pak3* Signaling Pathway to Regulate the Differentiation of Interneurons**

Since the ectopically distributed CR-positive interneurons in the mutants exhibited an enhanced dendritic branches (Fig. 2G' and H'), we suspected that *Foxg1* might regulate the postnatal differentiation of interneurons. Cell-based assays were then performed. First, we examined the number of neurites at 3 DIV and found that mutant interneurons exhibited enhanced dendrite growth (Fig. 5A and B). The total dendrite length was

significantly increased (Fig. 5E), but no obvious difference was detected in the length of the longest process (Fig. 5F). A Sholl analysis (Sholl 1953; Petilla Interneuron Nomenclature et al. 2008) was performed to further analyze the dendritic complexity. As shown in Figure 5I, dendritic complexity was significantly increased in mutants. At 7 DIV, the time at which cultured neurons are considered to be mature, mutant interneurons exhibited similar defects with that observed at 3 DIV (Fig. 5C,D,G,H,J). Thus, the postnatal ablation of *Foxg1* resulted in abnormal differentiation by enhancing the dendritic complexity of cortical interneurons.

Previously *Dlx1* has been shown to directly regulate interneuron dendrite growth (Cobos et al. 2007; Dai et al. 2014). *Dlx1* deficiency leads to upregulation of *Pak3* and increases the complexity of dendrites in vitro (Dai et al. 2014). A significant decreased transcriptional level of *Dlx1* was detected in our mutants. Consequently, the *Pak3* mRNA level was remarkably increased. This result was further confirmed at the protein levels by western blotting (Fig. 5K-L). We then performed the rescue experiments by overexpression of *Dlx1* and knock down of *Pak3*. Lentivirus carrying *Dlx1* cDNA fragment or *Pak3* shRNA was transformed into cultured interneurons respectively (Fig. 5M-P). Both overexpressing *Dlx1* and knock down *Pak3* could decrease the dendritic total length in mutant interneurons (Fig. 5Q-T). While, overexpression of *Dlx1* seemed to have stronger rescue effects compared with knock down of *Pak3* (Fig. 5R,T). Thus, *Foxg1* postnatally repressed the growth of cortical interneuron dendrites through the *Dlx1*-*Pak3* signaling pathway. The increased complexity of interneuron dendrites may also contribute to the migration defects in *Foxg1*-deficient interneurons.

***Foxg1* Deletion Increases the Epilepsy Susceptibility**

The abnormal distribution and decreased number of cortical interneurons observed in mutants are predicted to impair the neural circuits. To detect the ratio of interneurons among total cortical neurons, the *Gad67-GFP* reporter line was introduced to label interneurons. Total cortical neuron was viewed by immunostaining of anti-NeuN. We found that the percentage was decreased to 13.3% in *Gad67-GFP; Gad2-Cre^{ER}; Foxg1^{fl/fl}* mutants compared with 16.9% in the *Gad67-GFP; Foxg1^{fl/fl}* controls (Fig. 6A-E), indicating an imbalance of the neural circuit. We next examined the susceptibility of epilepsy induced by pentylenetetrazole (PTZ) (Ferraro et al. 1999; Naydenov et al. 2014). As shown in Figure 6F, the latency of the global tonic-clonic (GTC) seizures was dramatically shortened, although no significant differences of the latency of the partial clonus (PC) and generalized clonus (GC) were observed. Moreover, 63.63% of mutants died after GTC seizures compared with 15.38% of the controls (Fig. 6G). To further evaluate the epilepsy susceptibility more objectively, the weighting factor was considered to calculate the seizure scores, which could reflect the degree of progression of the seizure in each mouse (Naydenov et al. 2014). The mutants exhibited an increased severity of seizure behaviors, with a comparatively higher score of 1.58 (Fig. 6H). Our results, to certain extent, may explain why 75% of patients with a *Foxg1* mutation have epilepsy (Roche Martinez et al. 2011).

Discussion

Although interneurons represent only 15–20% of the cortical neurons, the integration of cortical interneurons into the circuits has been proven to be critical for the cortical network

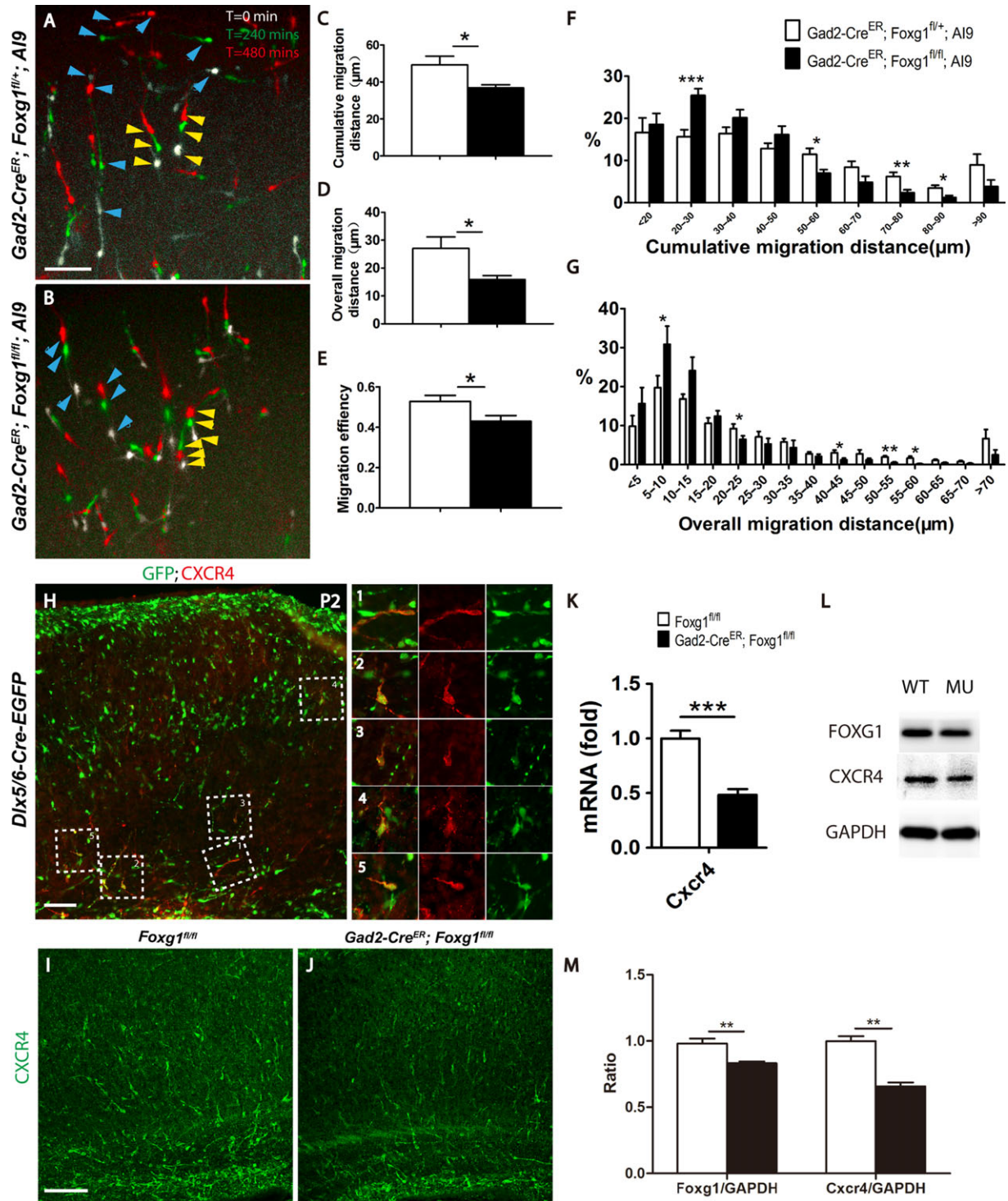


Figure 4. The ablation of *Foxg1* resulted in a decreased migration capacity. (A–B) Merge of 3 images of cultured P2 cortical slices showing the time-lapsed movement of interneurons within 480 min. White indicates the location of cells when the observation starts ($t = 0$ min), green indicates after 240 mins, the location where migrating cells migrated to, and red indicates the final location of migrating cells after 480 mins. Three aligned arrowheads indicate the migrating direction of each interneuron. Blue arrowheads represent the long-distance migrating cells and the yellow arrowheads represent the short-distance migrating cells. (A) The control interneurons migrated a longer distance. (B) The mutant interneurons. (C–E) Histograms of the cumulative (C; Control $n = 1282$ neurons from 9 slices, Mu, $n = 1087$ neurons from 8 slices; $P = 0.0317$) and overall (D, $P = 0.0270$) migration distances and the migration efficiency (E, $P = 0.0317$). (F–G) Distribution of the percentages of cumulative (F, 20–30 μm , $P = 0.0006$; 50–60 μm , $P = 0.0161$; 70–80 μm , $P = 0.0068$; 80–90 μm , $P = 0.0135$) and overall (G, 5–10 μm , $P = 0.043$; 20–25 μm , $P = 0.0485$; 40–45 μm , $P = 0.0381$; 50–55 μm , $P = 0.0013$; 55–60 μm , $P = 0.013$) migration of P2 interneurons. (H) Immunostaining on P2 cortex revealed that CXCR4 was expressed in interneurons on the tangential migrating stream (H-1) and the radial migrating interneurons (H2–H5). (I–J) Immunostaining revealed decreased CXCR4 expression level in the mutant (J) compared with that of the control (I). Q-PCR (K; Control, $n = 5$; MU, $n = 4$; $P = 0.0004$) and western blot analyses of Foxg1 and CXCR4 (L). (M) The comparative analysis of Foxg1 and CXCR4 at protein level ($n = 4$, $P = 0.006$). Scale bar: 100 μm in A, B, H, I; 50 μm in L–M. Student's t -test, * $P < 0.05$, ** $P < 0.01$, *** $P < 0.001$.

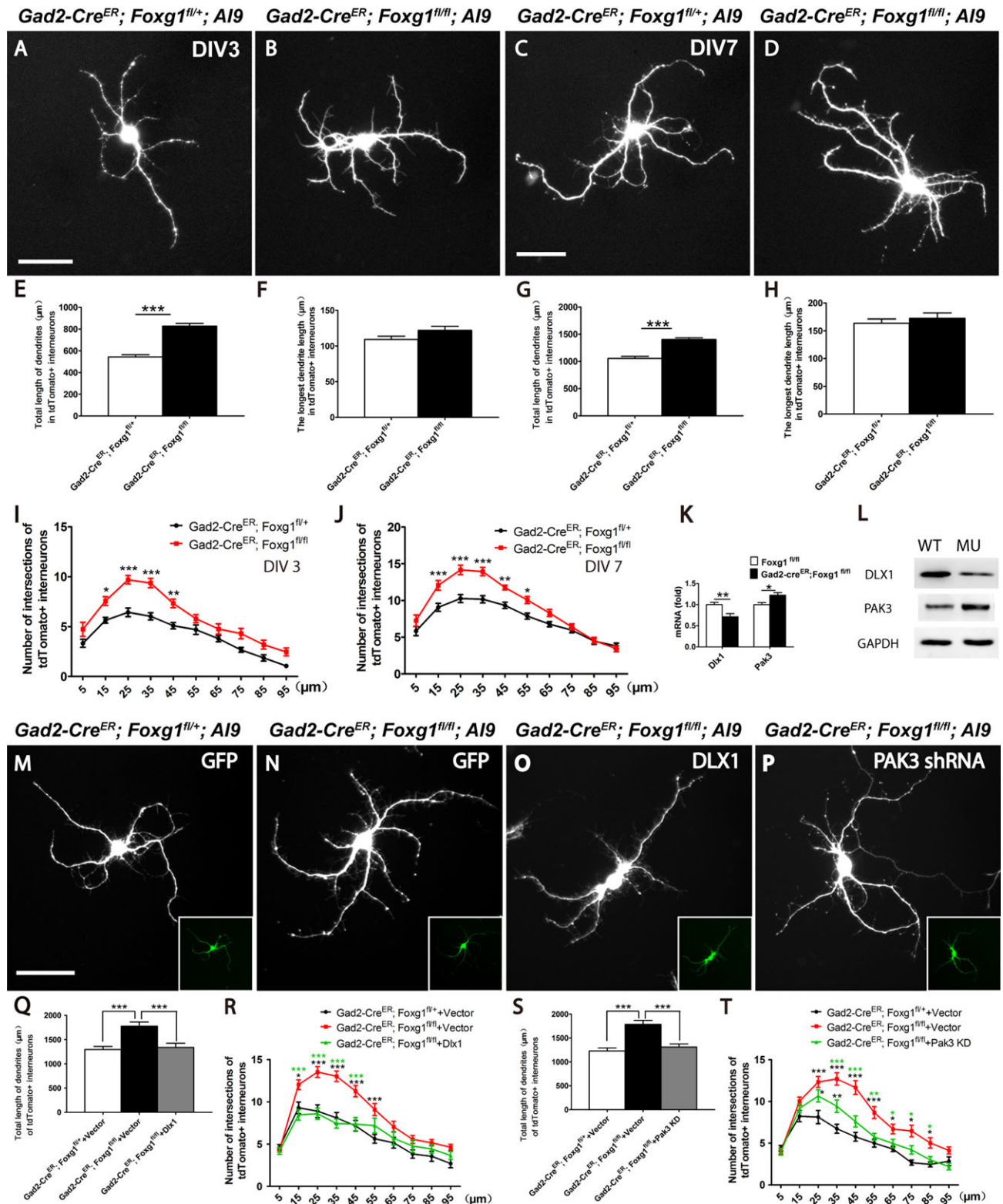


Figure 5. *Foxg1* restricted the growth of cortical interneuron dendrites. (A–B) Representative micrographs of tdTomato⁺ interneurons from the controls (A) and mutants (B) at 3 DIV showing enhanced dendritic complexity of the mutant interneurons. (C–D) Representative micrographs of tdTomato⁺ interneurons from the controls (C) and mutants (D) at 7 DIV show that the dendritic complexity further increased in the mutants. (E) The total dendrite length in the mutant interneurons was increased at 3 DIV compared with that in the controls (Control, $n = 30$; Mu $n = 31$; $P = 4.83756E^{-12}$). (F) No changes in the length of the longest neurite were detected between the mutants and controls at 3 DIV (Control, $n = 30$; Mu $n = 31$; $P = 0.087$). (G) The total length of mutant interneuron dendrites was remarkably increased at 7 DIV compared with 3 DIV (Control, $n = 30$; Mu $n = 30$; $P = 2.11852E^{-09}$). (H) No changes in the length of the longest neurite were detected between mutants and controls at 7 DIV (Control, $n = 30$; Mu $n = 30$; $P = 0.4779$). (I) Sholl analysis of the numbers of dendritic branches in tdTomato⁺ interneurons from the mutants and the controls at 3 DIV. ($n = 30$, two-way ANOVA ($F_{9, 522} = 2.211$, $P < 0.0001$) with Bonferroni's post hoc test, $P < 0.05$ at 15, 25, 35 and 45 μm away from the cell body). (J) The same

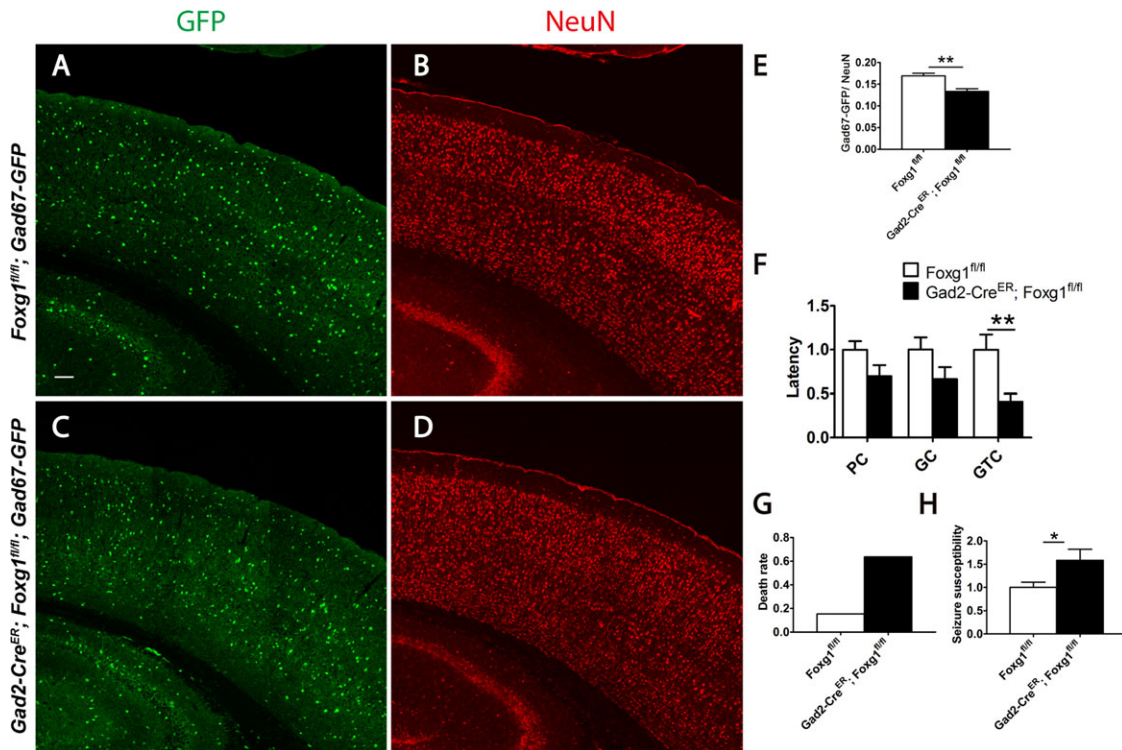


Figure 6. A neural circuit imbalance and increased epileptic susceptibility in the Foxg1-deficient mice. (A–D) GFP-labeled interneurons (A, C) and immunostaining of anti-NeuN viewed total neurons (B, D). (E) The ratio of interneurons to total neurons was decreased in adults (Control, $n = 13$; Mu, $n = 11$; $P = 0.0098$). (F–H) The latencies of stage 2–4 seizures (F; Control, $n = 13$; Mu, $n = 11$; latency of GTC, $P = 0.0086$) after PTZ induction, the death rate (G) and the seizure score was analyzed and calculated from the latencies (H; Control, $n = 13$; Mu, $n = 11$; $P = 0.0256$). Scale bar: 100 μm . Student's t -test, * $P < 0.05$, ** $P < 0.01$.

(Kann 2016). Cortical interneurons are a highly heterogeneous group with distinct subtypes located in specific positions in the cortex. The final distributions of cortical interneurons require not only a normal switch from the tangential to radial migration to avoid an accumulation in the migration streams or premature integration into the cortex, but also the proper migration capacity and the accurate timing to terminate the migration. However, the mechanism underlying postnatal development has not been fully revealed. Here, by employing the *Gad2-Cre^{ER}* line, we postnatally deleted *Foxg1* in interneurons and observed a decreased migration capacity in cortical interneurons and abnormal distributions of interneurons subtypes. Furthermore, *Foxg1*-deficient cortical interneurons showed an increased dendritic complexity, suggesting severe differentiation defects. As a consequence of unbalanced neural circuit, increased epilepsy susceptibility was observed in mutant mice. Our study will improve understanding of the regulation of postnatal development of cortical interneurons and offer insights into the mechanisms underlying Foxg1-related disorders.

In our mutants, the laminar distribution of interneuron subtypes, such as SST-, CR-, and NPY-positive interneurons, was disrupted. Ectopic accumulation of SST-positive interneurons in the superficial layers, NPY-positive interneurons in the layer IV, and CR-positive interneurons in the deeper layers (including the intermediate zone (IZ)/subventricular zone (SVZ)) was observed. Interneurons migrate toward their destinations under the guidance of extracellular cues (Pla et al. 2006; Lodato et al. 2011). Previously it has been reported ablation of CXCR4 results in abnormal distributions of subtypes of SST-, NPY- and CR-positive interneurons in the cortex. After *Foxg1* deletion significant downregulation of CXCR4 was observed here, suggested a potential role of Foxg1 functioning upstream of CXCR4 in the postnatal development of cortical neurons. Impaired neurite development was also observed in our mutants. The total length and complexity of the dendrites was remarkably increased. Previous studies have shown exogenous expression of *Dlx1* resulted in reduced complexity of dendritic arborization, and knock down of *Dlx1* enhanced dendritic growth

result was obtained when the Sholl analysis of the dendritic branches was performed at 7 DIV ($n = 30$, compared by two-way ANOVA ($F_{9, 622} = 5.174$, $P < 0.0001$) with Bonferroni's post hoc test, $P < 0.05$ at 15, 25, 35, 45, and 55 μm away from the cell body). (K–L) Levels of the *Dlx1* and *Pak3* mRNAs (K) and proteins (L). (M–P) Representative micrographs of tdTomato⁺ interneurons from the controls (M) and mutants (N) transfected with empty vector, mutants transfected with lentivirus carrying *Dlx1* cDNA (N) and *Pak3* shRNA (O) at 7 DIV showing that enhanced dendritic complexity of the mutant interneurons can be rescued. (Q–T) Both *Dlx1* overexpression (Q) and the *Pak3* knock down (S) decrease the total length of mutant dendrites (For *Dlx1*, $n = 30$, analyzed by one-way ANOVA ($F_{2, 89} = 11.29$, $P < 0.0001$) with Bonferroni's post hoc test, $P < 0.001$ between mutant and control, mutant and mutant-*dlx1* overexpression; For *Pak3* shRNA $n = 30$, analyzed by one-way ANOVA ($F_{2, 89} = 18.15$, $P < 0.0001$) with Bonferroni's post hoc test, $P < 0.001$ between mutant and control, mutant and mutant-*Pak3* shRNA). (R, T) Sholl analysis revealed that overexpression of *Dlx1* ($n = 30$, analyzed by two-way ANOVA ($F_{18, 870} = 3.281$, $P < 0.0001$) with Bonferroni's post hoc test, for control and mutant, $P < 0.05$ at 15, 25, 35, 45 and 55 μm away from the cell body (black asterisk), for mutant-*Dlx1* and mutant, $P < 0.05$ at 15, 25, 35, and 45 μm away from the cell body (green asterisk)) has stronger effects than *Pak3* shRNA ($n = 30$, analyzed by two-way ANOVA ($F_{18, 870} = 3.281$, $P < 0.0001$) with Bonferroni's post hoc test, for control and mutant, $P < 0.05$ at 25–85 μm away from the cell body (black asterisk), for mutant-*Pak3* shRNA and mutant, $P < 0.05$ at 35–85 μm away from the cell body (green asterisk), for mutant-*Pak3* shRNA and control, $P < 0.05$ at 25 and 35 μm away from the cell body (black asterisk)). Scale bar: 50 μm . Student's t -test, * $P < 0.05$, ** $P < 0.01$, *** $P < 0.001$.

(Dai et al. 2014). In *Dlx1^{-/-}*; *Dlx2^{-/-}* mutants, neurite length is increased and cells fail to migrate (Cobos et al. 2007). These results are consistent with what we have observed here. In this study, *Dlx1* expression was severely downregulated, subsequently leading to an upregulation of Pak3 and an ultimate increase in enhanced dendritic complexity. Based on these results, we conclude that *Foxg1* functions as an upstream regulator of CXCR4 and *Dlx1* to control the postnatal development of cortical interneurons.

The transition from tangential to radial migration has been shown to be indispensable for interneuron development (Azim et al. 2009; Batista-Brito et al. 2009; Caronia-Brown and Grove 2011; Sanchez-Alcaniz et al. 2011). However, we could not examine the switch from tangential to radial migration in this study due to the deletion of *Foxg1* induced by tamoxifen administration occurred after the transition was almost completed, and no obvious accumulation of interneurons was detected in the 2 tangential streams in the marginal zone (MZ) or SVZ. Further studies using an appropriate Cre mouse tool are required to determine whether *Foxg1* functions in this process.

Although most cortical interneurons are produced in the MGE and the CGE during embryonic development, the existence of an extra source of cortical interneurons, such as the white matter, has been reported. A portion of CR-positive interneurons are produced there during the first postnatal week and migrate to the cortex (Ricchio et al. 2012). Previous studies also have shown that olfactory bulb interneurons were continuously generated after birth and migrate to their destinations alone RMS (Lledo et al. 2008; Brill et al. 2009). Interestingly, we observed a group of CR-positive cells that were ectopically accumulated in the deeper layer of the cortex, and these cells were produced postnatally. These interneurons might be either cortical interneurons or olfactory bulb interneurons. The abnormal accumulation of CR-positive cells in the deeper layers of the cortex is also reported in CXCR4 cKO mice (Li et al. 2008). Considering the downregulation of CXCR4 expression in our *Foxg1*-deficient interneurons, *Foxg1* may function upstream of CXCR4 to regulate the development of postnatally born CR-positive interneurons.

Mutations in *Foxg1* have been identified in patients with Rett syndrome and West syndrome (Das et al. 2014; Takahashi 2014). Recently, *Foxg1*-related clinical symptoms were defined as *Foxg1* syndrome (Kortum et al. 2011; Pratt et al. 2013). Most patients carrying *Foxg1* mutations experience seizures, which are the consequence of an imbalanced neural circuit that exhibits reduced GABAergic inhibition (Roche Martinez et al. 2011; Matsui and Hsieh 2016). Our *Foxg1* mutant mice exhibited increased epilepsy susceptibility, which may be a direct consequence of the decreased number and impaired distribution of interneurons. Our study explained, to a certain extent, why patients with *Foxg1* syndrome have a high incidence of seizures. Previously, we have reported that at embryonic stages *Foxg1* regulates the tangential migration of cortical interneurons. In this study, by postnatal deletion *Foxg1* we have found the laminar distribution of subtypes of interneurons, including SST-, NPY-, and CR-positive interneurons were impaired. However, subtypes of the PV-, VIP-, and Reelin-positive interneurons did not exhibit an abnormal distribution, possibly due to the time point of tamoxifen induction is not critical for these subtypes. Another possibility is *Foxg1* plays different roles in distinct interneuron subtypes. Further studies are needed to reveal the function of *Foxg1* in distinct interneuron subtypes.

Funding

This work was supported by grant 2016YFA0501001 from the Ministry of Science and Technology of the People's Republic of

China, the National Natural Science Foundation of China (Grants 91232301 and 31471041 to C.Z. and Grants 91632201 to W.X.).

Notes

We would like to thank Professor Yuchio Yanagawa at Gunma University for providing the *Gad67-GFP* mice, Professor Xiaoming Li at Zhejiang University for providing the Ai9 mice, Professor Zhengang Yang at Fudan University for providing the *Dlx5/6-cre-EGFP* mice, Mr. Yiquan Wei and Ms. Li Liu for their assistance with laboratory and animal care and other members of the laboratory for discussion. *Competing Interests:* The authors have no conflicts of interest to declare.

References

- Anderson SA, Marin O, Horn C, Jennings K, Rubenstein JL. 2001. Distinct cortical migrations from the medial and lateral ganglionic eminences. *Development*. 128:353–363.
- Ang ES Jr, Haydar TF, Gluncic V, Rakic P. 2003. Four-dimensional migratory coordinates of GABAergic interneurons in the developing mouse cortex. *J Neurosci*. 23:5805–5815.
- Azim E, Jabaudon D, Fame RM, Macklis JD. 2009. SOX6 controls dorsal progenitor identity and interneuron diversity during neocortical development. *Nat Neurosci*. 12:1238–1247.
- Bartolini G, Ciceri G, Marin O. 2013. Integration of GABAergic interneurons into cortical cell assemblies: lessons from embryos and adults. *Neuron*. 79:849–864.
- Batista-Brito R, Rossignol E, Hjerling-Leffler J, Denaxa M, Wegner M, Lefebvre V, Pachnis V, Fishell G. 2009. The cell-intrinsic requirement of Sox6 for cortical interneuron development. *Neuron*. 63:466–481.
- Brill MS, Ninkovic J, Winpenny E, Hodge RD, Ozen I, Yang R, Lepier A, Gascon S, Erdelyi F, Szabo G, et al. 2009. Adult generation of glutamatergic olfactory bulb interneurons. *Nat Neurosci*. 12:1524–1533.
- Butt SJ, Fuccillo M, Nery S, Noctor S, Kriegstein A, Corbin JG, Fishell G. 2005. The temporal and spatial origins of cortical interneurons predict their physiological subtype. *Neuron*. 48:591–604.
- Caronia-Brown G, Grove EA. 2011. Timing of cortical interneuron migration is influenced by the cortical hem. *Cereb Cortex*. 21:748–755.
- Chen B, Wang SS, Hattox AM, Rayburn H, Nelson SB, McConnell SK. 2008. The *Fezf2-Ctip2* genetic pathway regulates the fate choice of subcortical projection neurons in the developing cerebral cortex. *Proc Natl Acad Sci USA*. 105:11382–11387.
- Cobos I, Borello U, Rubenstein JL. 2007. *Dlx* transcription factors promote migration through repression of axon and dendrite growth. *Neuron*. 54:873–888.
- Dai X, Iwasaki H, Watanabe M, Okabe S. 2014. *Dlx1* transcription factor regulates dendritic growth and postsynaptic differentiation through inhibition of neuropilin-2 and PAK3 expression. *Eur J Neurosci*. 39:531–547.
- Das DK, Jadhav V, Ghattargi VC, Udani V. 2014. Novel mutation in forkhead box G1 (*FOXG1*) gene in an Indian patient with Rett syndrome. *Gene*. 538:109–112.
- Faux C, Rakic S, Andrews W, Britto JM. 2012. Neurons on the move: migration and lamination of cortical interneurons. *Neurosignals*. 20:168–189.
- Ferraro TN, Golden GT, St Smith GG, Jean P, Schork NJ, Mulholland N, Ballas C, Schill J, Buono RJ, Berrettini WH. 1999. Mapping loci for pentylentetrazol-induced seizure susceptibility in mice. *J Neurosci*. 19:6733–6739.

- Gelman DM, Marin O. 2010. Generation of interneuron diversity in the mouse cerebral cortex. *Eur J Neurosci*. 31:2136–2141.
- Guo S, Palanski BA, Kloeck C, Khosla C, Cui B. 2017. Intracellular TG2 activity increases microtubule stability but is not sufficient to prompt neurite growth. *Neurosci Bull*. 33:103–106.
- Hu Y, Li S, Jiang H, Li MT, Zhou JW. 2014. Ephrin-B2/EphA4 forward signaling is required for regulation of radial migration of cortical neurons in the mouse. *Neurosci Bull*. 30:425–432.
- Inamura N, Kimura T, Tada S, Kurahashi T, Yanagida M, Yanagawa Y, Ikenaka K, Murakami F. 2012. Intrinsic and extrinsic mechanisms control the termination of cortical interneuron migration. *J Neurosci*. 32:6032–6042.
- Jimenez D, Lopez-Mascaraque LM, Valverde F, De Carlos JA. 2002. Tangential migration in neocortical development. *Dev Biol*. 244:155–169.
- Kann O. 2016. The interneuron energy hypothesis: implications for brain disease. *Neurobiol Dis*. 90:75–85.
- Kortum F, Das S, Flindt M, Morris-Rosendahl DJ, Stefanova I, Goldstein A, Horn D, Klopocki E, Kluger G, Martin P, et al. 2011. The core FOXG1 syndrome phenotype consists of postnatal microcephaly, severe mental retardation, absent language, dyskinesia, and corpus callosum hypogenesis. *J Med Genet*. 48:396–406.
- Li G, Adesnik H, Li J, Long J, Nicoll RA, Rubenstein JL, Pleasure SJ. 2008. Regional distribution of cortical interneurons and development of inhibitory tone are regulated by Cxcl12/Cxcr4 signaling. *J Neurosci*. 28:1085–1098.
- Liu J, Liu B, Zhang X, Yu B, Guan W, Wang K, Yang Y, Gong Y, Wu X, Yanagawa Y, et al. 2014. Calretinin-positive L5a pyramidal neurons in the development of the paralemniscal pathway in the barrel cortex. *Mol Brain*. 7:84.
- Lledo PM, Merkle FT, Alvarez-Buylla A. 2008. Origin and function of olfactory bulb interneuron diversity. *Trends Neurosci*. 31:392–400.
- Lodato S, Rouaux C, Quast KB, Jantrachotechatchawan C, Studer M, Hensch TK, Arlotta P. 2011. Excitatory projection neuron subtypes control the distribution of local inhibitory interneurons in the cerebral cortex. *Neuron*. 69:763–779.
- Martini FJ, Valiente M, Lopez Bendito G, Szabo G, Moya F, Valdeolmillos M, Marin O. 2009. Biased selection of leading process branches mediates chemotaxis during tangential neuronal migration. *Development*. 136:41–50.
- Matsui T, Hsieh J. 2016. GABAergic interneurons-in-a-dish: high five for epilepsy. *Epilepsy Curr*. 16:177–178.
- Meechan DW, Tucker ES, Maynard TM, LaMantia AS. 2012. Cxcr4 regulation of interneuron migration is disrupted in 22q11.2 deletion syndrome. *Proc Natl Acad Sci USA*. 109:18601–18606.
- Meyer HS, Schwarz D, Wimmer VC, Schmitt AC, Kerr JN, Sakmann B, Helmstaedter M. 2011. Inhibitory interneurons in a cortical column form hot zones of inhibition in layers 2 and 5A. *Proc Natl Acad Sci USA*. 108:16807–16812.
- Miyoshi G, Butt SJ, Takebayashi H, Fishell G. 2007. Physiologically distinct temporal cohorts of cortical interneurons arise from telencephalic Olig2-expressing precursors. *J Neurosci*. 27:7786–7798.
- Miyoshi G, Fishell G. 2011. GABAergic interneuron lineages selectively sort into specific cortical layers during early postnatal development. *Cereb Cortex*. 21:845–852.
- Miyoshi G, Hjerling-Leffler J, Karayannis T, Sousa VH, Butt SJ, Battiste J, Johnson JE, Machold RP, Fishell G. 2010. Genetic fate mapping reveals that the caudal ganglionic eminence produces a large and diverse population of superficial cortical interneurons. *J Neurosci*. 30:1582–1594.
- Naydenov AV, Horne EA, Cheah CS, Swinney K, Hsu KL, Cao JK, Marrs WR, Blankman JL, Tu S, Cherry AE, et al. 2014. ABHD6 blockade exerts antiepileptic activity in PTZ-induced seizures and in spontaneous seizures in R6/2 mice. *Neuron*. 83:361–371.
- Petilla Interneuron Nomenclature Group, Ascoli GA, Alonso-Nanclares L, Anderson SA, Barrionuevo G, Benavides-Piccione R, Burkhalter A, Buzsaki G, Cauli B, Defelipe J, Fairen A, et al. 2008. Petilla terminology: nomenclature of features of GABAergic interneurons of the cerebral cortex. *Nat Rev Neurosci*. 9:557–568.
- Pla R, Borrell V, Flames N, Marin O. 2006. Layer acquisition by cortical GABAergic interneurons is independent of Reelin signaling. *J Neurosci*. 26:6924–6934.
- Pratt DW, Warner JV, Williams MG. 2013. Genotyping FOXG1 mutations in patients with clinical evidence of the FOXG1 syndrome. *Mol Syndromol*. 3:284–287.
- Riccio O, Murthy S, Szabo G, Vutskits L, Kiss JZ, Vitalis T, Lebrand C, Dayer AG. 2012. New pool of cortical interneuron precursors in the early postnatal dorsal white matter. *Cereb Cortex*. 22:86–98.
- Roche Martinez A, Alonso Colmenero MI, Gomes Pereira A, Sanmarti Vilaplana FX, Armstrong Moron J, Pineda Marfa M. 2011. Reflex seizures in Rett syndrome. *Epileptic Disord*. 13:389–393.
- Rymar VV, Sadikot AF. 2007. Laminal fate of cortical GABAergic interneurons is dependent on both birthdate and phenotype. *J Comp Neurol*. 501:369–380.
- Sanchez-Alcaniz JA, Haegel S, Mueller W, Pla R, Mackay F, Schulz S, Lopez-Bendito G, Stumm R, Marin O. 2011. Cxcr7 controls neuronal migration by regulating chemokine responsiveness. *Neuron*. 69:77–90.
- Sholl DA. 1953. Dendritic organization in the neurons of the visual and motor cortices of the cat. *J Anat*. 87:387–406.
- Stumm R, Kolodziej A, Schulz S, Kohtz JD, Holt V. 2007. Patterns of SDF-1alpha and SDF-1gamma mRNAs, migration pathways, and phenotypes of CXCR4-expressing neurons in the developing rat telencephalon. *J Comp Neurol*. 502:382–399.
- Stumm RK, Zhou C, Ara T, Lazarini F, Dubois-Dalcq M, Nagasawa T, Holt V, Schulz S. 2003. CXCR4 regulates interneuron migration in the developing neocortex. *J Neurosci*. 23:5123–5130.
- Takahashi S. 2014. [Clinical features in Rett syndrome: MECP2-, CDKL5- and FOXG1- related disorders]. *No To Hattatsu*. 46:117–120.
- Tamamaki N, Yanagawa Y, Tomioka R, Miyazaki J, Obata K, Kaneko T. 2003. Green fluorescent protein expression and colocalization with calretinin, parvalbumin, and somatostatin in the GAD67-GFP knock-in mouse. *J Comp Neurol*. 467:60–79.
- Tanaka D, Nakaya Y, Yanagawa Y, Obata K, Murakami F. 2003. Multimodal tangential migration of neocortical GABAergic neurons independent of GPI-anchored proteins. *Development*. 130:5803–5813.
- Tanaka DH, Maekawa K, Yanagawa Y, Obata K, Murakami F. 2006. Multidirectional and multizonal tangential migration of GABAergic interneurons in the developing cerebral cortex. *Development*. 133:2167–2176.
- Tanaka DH, Mikami S, Nagasawa T, Miyazaki J, Nakajima K, Murakami F. 2010. CXCR4 is required for proper regional and laminar distribution of cortical somatostatin-, calretinin-, and neuropeptide Y-expressing GABAergic interneurons. *Cereb Cortex*. 20:2810–2817.
- Tanaka DH, Yanagida M, Zhu Y, Mikami S, Nagasawa T, Miyazaki J, Yanagawa Y, Obata K, Murakami F. 2009.

- Random walk behavior of migrating cortical interneurons in the marginal zone: time-lapse analysis in flat-mount cortex. *J Neurosci.* 29:1300–1311.
- Tian C, Gong Y, Yang Y, Shen W, Wang K, Liu J, Xu B, Zhao J, Zhao C. 2012. *Foxg1* has an essential role in postnatal development of the dentate gyrus. *J Neurosci.* 32:2931–2949.
- Tiveron MC, Rossel M, Moepps B, Zhang YL, Seidenfaden R, Favor J, Konig N, Cremer H. 2006. Molecular interaction between projection neuron precursors and invading interneurons via stromal-derived factor 1 (CXCL12)/CXCR4 signaling in the cortical subventricular zone/intermediate zone. *J Neurosci.* 26:13273–13278.
- Valcanis H, Tan SS. 2003. Layer specification of transplanted interneurons in developing mouse neocortex. *J Neurosci.* 23:5113–5122.
- Vucurovic K, Gallopin T, Ferezou I, Rancillac A, Chameau P, van Hooft JA, Geoffroy H, Monyer H, Rossier J, Vitalis T. 2010. Serotonin 3A receptor subtype as an early and protracted marker of cortical interneuron subpopulations. *Cereb Cortex.* 20:2333–2347.
- Wang Y, Li G, Stanco A, Long JE, Crawford D, Potter GB, Pleasure SJ, Behrens T, Rubenstein JL. 2011. CXCR4 and CXCR7 have distinct functions in regulating interneuron migration. *Neuron.* 69:61–76.
- Wonders CP, Taylor L, Welagen J, Mbata IC, Xiang JZ, Anderson SA. 2008. A spatial bias for the origins of interneuron subgroups within the medial ganglionic eminence. *Dev Biol.* 314:127–136.
- Xu X, Callaway EM. 2009. Laminar specificity of functional input to distinct types of inhibitory cortical neurons. *J Neurosci.* 29:70–85.
- Yang Y, Shen W, Ni Y, Su Y, Yang Z, Zhao C. 2017. Impaired Interneuron Development after *Foxg1* Disruption. *Cereb Cortex.* 27:793–808.
- Zhao C, Guan W, Pleasure SJ. 2006. A transgenic marker mouse line labels Cajal-Retzius cells from the cortical hem and thalamocortical axons. *Brain Res.* 1077:48–53.